ACS ES&T Water

pubs.acs.org/estwater

Article

Fluorescence and Absorbance Indices for Dissolved Organic Matter from Wildfire Ash and Burned Watersheds

Sarah J. Fischer,* Timothy S. Fegel, Paul J. Wilkerson, Leah Rivera, Charles C. Rhoades, and Fernando L. Rosario-Ortiz*

Cite This: *ACS EST Water* 2023, 3, 2199–2209

Read Online

ACCESS | Metrics & More | Article Recommendations | Supporting Information

ABSTRACT: Wildfires generate significant amounts of ash and burned soils that can leach altered dissolved organic matter (DOM) to watersheds. In this work, we analyzed the absorbance and fluorescence spectrum of DOM leached from 40 ash and soil samples collected from two conifer forest burn scars. DOM fluorescence quantum yield at 350 nm (ϕ_{f350}) was elevated in all ash and burned soil leachates. Wildfire DOM fluorescence was also consistently shifted toward the ultraviolet (UV) region relative to unburned materials, which limited the utility of several pre-defined optical indices, such as the humification index (HIX) and $SUVA_{254}$, for wildfire DOM differentiation. In contrast, E_2:E_3 and ϕ_{f350} resolved differences between ash, burned mineral soil, and unburned soil DOM across an assortment of physical settings. Mixtures of a freshwater DOM reference material and wildfire ash leachate confirmed that specific fluorescence peaks A and C, ϕ_{f350}, and E_2:E_3 were well correlated ($R^2 > 0.92$) to mass increases of ash-derived DOM. These findings were compared to 31 surface water samples collected from burned tributaries within the Cameron Peak Fire burnscar. Surface waters draining from the burn scar were also elevated in ϕ_{f350}, E_2:E_3, $SUVA_{254}$, FI, and UV-shifted fluorescence peaks A and C at intensities comparable to ash mixing experiments.

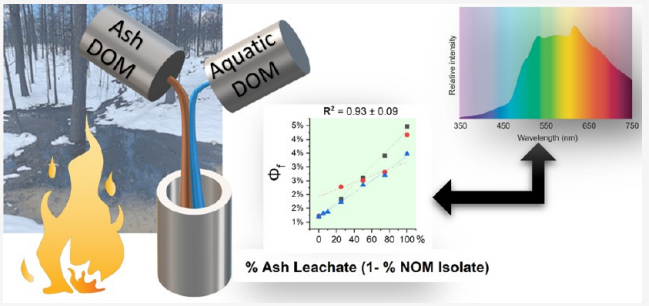

KEYWORDS: *wildfire ash, optical metrics, $SUVA_{254}$, absorbance spectroscopy, excitation−emission matrix, wildfire chemistry*

1. INTRODUCTION

Wildfires are a natural part of many forested and grassland ecosystems that have lasting impacts on watersheds and water quality.[1,2] The past century of climate change, fuel buildup, and fire suppression increased the frequency, size, and severity of wildfires across the western US.[1,3,4] In recent years, some of the largest wildfires ever recorded have occurred in California and Colorado. Forest fires are expected to continue to increase in frequency and size in upcoming decades.

Forested watersheds are also the primary source of residential, industrial, and agricultural water supplies in the US.[5] Wildfires significantly impact watersheds by combusting vegetation and soils, generating large quantities of ash, and altering hydrology.[6,7] Ash and burned soil mobilize during rain and snowmelt, which creates numerous challenges for drinking water providers.[4] For example, post-wildfire turbidity reduces filtration and coagulation treatment efficiency.[3,8,9] Drinking water disinfection can also be impacted by wildfire-derived dissolved organic matter (DOM).[7,9−11] Recent work demonstrates both regulated carbonaceous and unregulated nitrogenous disinfection byproducts (DBPs) formation potential can be altered due to wildfire-derived DOM.[10] These water quality issues increase the need for reliable monitoring strategies of burned organic matter in impacted watersheds.

Bulk DOM quality can generally be tracked via optical properties and predefined optical indices that target portions of spectra. Dozens of optical metrics or excitation−emission couples targeting colored or fluorescent DOM have been well described in reviews by Fellman and Gabor.[13] However, most optical indices have been developed during the study of freshwater or marine DOM. Recent work has demonstrated that wildfires elevate the specific UV absorbance ($SUVA_{254}$) and fluorescence index (FI),[7,9,14,15] but limited justification exists for why these metrics were selected. Furthermore, limited work has focused on the defining characteristics of ash-derived DOM spectra and indices can best describe DOM originating from large, burned landscapes. Recent work tracked colored and fluorescent DOM (C/fDOM) changes of forest soil combusted over a range of muffle furnace temperatures up to 450 °C.[15] McKay et al. demonstrated that increases in $SUVA_{254}$, fluorescence quantum yield (ϕ_{f370}), and carbon-

Received: January 12, 2023
Revised: July 11, 2023
Accepted: July 11, 2023
Published: July 31, 2023

https://doi.org/10.1021/acsestwater.3c00017
ACS EST Water 2023, 3, 2199−2209

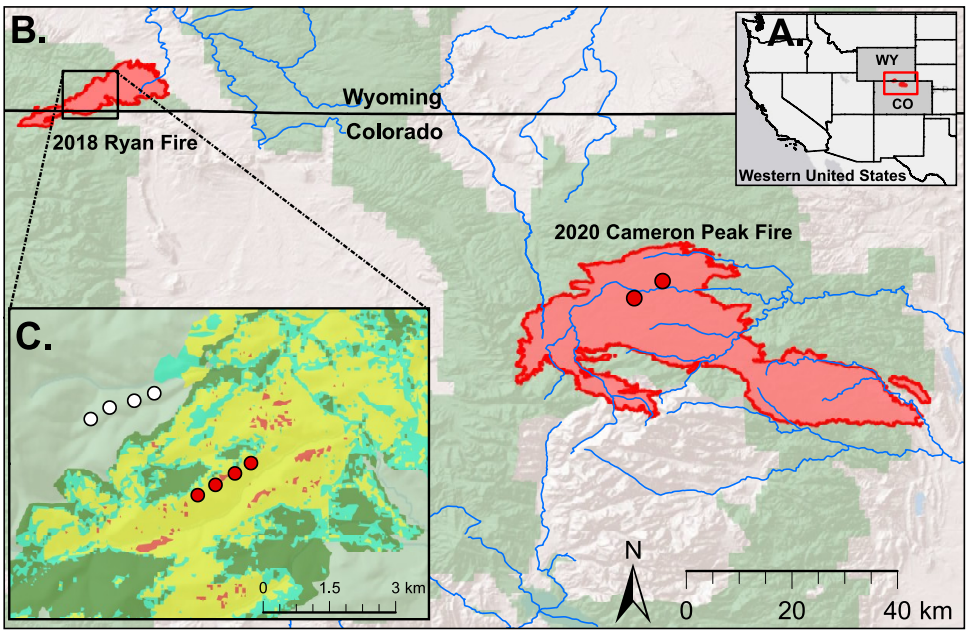

Figure 1. (A) Location of study burn scars in the Western United States, (B) 2018 Ryan and 2020 Cameron Peak fire perimeters (red) and sampling locations, and (C) Ryan Fire sample locations within areas of moderate (yellow) and high (red) soil burn severity. Red and white dots denote burned and unburned sample locations discussed in Table S1.

normalized fluorescence correlate to combustion temperature ($R^2 > 0.96$) that is consistent with increases in soluble aromatic carbon.[14,16] Muffle furnace experiments are homogeneous relative to wildfire activity, however. Less work has closely examined the range of possible optical properties of DOM derived from ash, burned soil, or surface waters of large, burned watersheds.

In large burns, ashes and soils are subject to a range of forest ages, oxygen availability, and temperatures that create spatial heterogeneity of burn severities and combustion conditions.[12,17] Limited work has attempted to systematically propose which optical indices work best for differentiating wildfire DOM from unimpacted DOM. Recent analysis of wastewater blends[18] and biosolid leachates[19] demonstrated that optical spectra of these materials significantly contrast aquatic DOM, and not all optical indices statistically capture these differences. Statistically robust measurement of wildfire-derived DOM may also require specific wavelength regions and metrics.

Therefore, the first goal of this study was to evaluate spectral properties and several predefined optical indices for wildfire-impacted DOM from a range of ash and soil collected in two recent wildfires in Colorado. Next, we determined the optical properties of wildfire-derived DOM and an aquatic isolate DOM blended in different ratios. We compared indices of $SUVA_{254}$, E_2:E_3, ϕ_f, humification index (HIX), fluorescence index (FI), specific fluorescence peaks A, B, T, and C, and peak ratios (A:C, C:T, and A:T) to evaluate which indices were highly correlated to mass increases in wildfire DOM. Lastly, we analyzed optical spectra qualities and indices of 31 surface water samples from the burned watershed where ash was also collected. Our aim was to assess the optical variability of wildfire DOM and assess which indices were statistically robust for detection of DOM originating from large, burned watersheds.

2. MATERIALS AND METHODS

2.1. Wildfire Descriptions and Sampling. The 2018 Ryan Fire burned 88 km^2 along the Colorado-Wyoming border and the 2020 Cameron Peak Fire burned 884 km^2 in the Cache La Poudre watershed west of Fort Collins, Colorado. Both fires burned primarily in subalpine forest dominated by lodgepole pine (*Pinus contorta*) and in mixtures of lodgepole pine with Engelmann spruce (*Picea engelmannii*) and subalpine fir (*Abies lasiocarpa*).

We collected 40 ash and soil samples from the two wildfires (Figure 1). Material from the Ryan Fire was collected in 2018 and 2019 (Table S1). The 2018 sampling occurred within a month of fire containment before the development of the winter snowpack. The second sampling was in September 2019 following snowmelt and summer rainstorms. Samples were collected in old-growth and second-growth forests in areas that burned at medium and high severity.[20] Burned mineral soils (0−10 cm depth) were collected after overlying ash and char were removed. At an unburned site outside the Ryan Fire perimeter (Figure 1), we sampled the organic (O-horizon) and then carefully removed residual O-horizon material and collected a 0−10 cm depth mineral soil sample. Ash and soils from a subset of sites were resampled in September 2019. Samples from the Cameron Peak fire were collected in November 2020 prior to significant precipitation in two watersheds in areas that burned at high and moderate severity (Table S1). Within the Cameron Peak fire, samples were collected from the Black Hollow Creek and Sevenmile Creek sub-catchments. No unburned soils were collected outside the burn scar at the time of CPF ash sampling due to logistical constraints, and mixing experiments were therefore conducted with a general aquatic DOM reference (Section 2.4), Upper Mississippi River Natural Organic Matter (MR NOM − Lot 1R110N). All wildfire ash and soil samples were stored in the dark at 4 °C prior to analysis.

2.2. Leaching of Ash and Soils. Ash and soils were passed through a 2 mm mesh stainless steel sieve to remove

https://doi.org/10.1021/acsestwater.3c00017
ACS EST Water 2023, 3, 2199−2209

rocks, roots, and sticks. Samples were dried at 40 °C overnight prior to analysis. Dried samples were stored in acid-washed and combusted glass vials until use. A 0.01 M $CaCl_2$ leaching solution was prepared in pre-cleaned glass bottles by dissolving >99% Trace Metal Grade ACS Reagent $CaCl_2$-$2H_2O$ into ultra-pure Type I DI water, following Gabor et al.[21] Dilute calcium chloride was chosen to model natural water ionic strength with low interference to optical spectroscopy.[21]

Preliminary kinetic experiments confirmed 1:10 (w/v) soil:ionic solution ratio and 16 or more hours were sufficient to extract a constant level of dissolved organic carbon (DOC) to steady-state concentrations (Section 2.3). Immediately before leaching, 4 g of dried sample was weighed in plastic weigh boats and placed in cleaned 50 mL centrifuge tubes with 40 mL of ionic solution. Sample mixtures were agitated on a VWR Analogue Standard Shaker at a moderate speed for 16 h. Mixtures were then centrifuged at a moderate speed for 10−15 min in a Thermo Scientific Sorvall Legend X1 centrifuge to draw down particulates and improve the filtration efficiency of the supernatant. The supernatant was filtered through a pre-rinsed 0.7 μM glass fiber filter (Whatman GD/X) to separate out DOM, which was quantified for dissolved organic carbon (DOC) content as described in Section 2.3. Filtered leachates were stored in combusted amber glass vials. The ionic leaching solution and filtered leachates were stored in dark refrigeration at 4 °C for up to 1 month before analytical measurements.

2.3. Dissolved Organic Carbon Quantification, pH, and Elemental Analysis of Solids. DOC of leachates was quantified to: (i) determine dissolved soluble carbon (C) per gram C in solids (Figure S1), (ii) normalize optical metrics based on carbon concentration ($SUVA_{254}$, Specific Peak A, C, and T, described in Section 2.5 and Table S3), and (iii) normalize bulk optical spectra to molar or carbon concentration. DOC of leachates was determined via a Sievers 5310 C Total Organic Carbon (TOC) analyzer (Boulder, CO) within 72 h after the leachates were created. The Sievers 5310 TOC was calibrated with a certified Potassium Phthalate standard over a range of 0−10 ppm (RICCA Chemical Company, Arlington, TX). Samples were automatically acidified via 2% hydrochloric acid to remove inorganic carbon in carbonates. Vials containing ultra-pure DI water were analyzed before and after every five samples to check for carryover. Additionally, three continuing calibration samples were analyzed to ensure instrument accuracy and precision staying within the laboratory's acceptable standard deviation of ±0.2 mg C/L. Dilutions of stock leachates were required to bring leachates into the calibration range of the Sievers 5310 C and Horiba Fluoromax F-4 (Kyoto, Japan). Any dilutions were made using 0.01 M $CaCl_2$ to keep the pH and ionic matrix constant throughout all measurements. The pH of 1:10 w/v extracted leachates was measured with an Orion glass fritted 8157 BNUM pH probe and Orion Versa Star Meter. The probe and meter were recalibrated by a 3-point calibration of fresh buffer. The C/N ratio and % C of soils and ashes were determined via an Elementar CHN Analyzer with ETDA standards, Center for Environmental Systems Analysis, CU Boulder. Ashes and soils were homogenized with a clean mortar and pestle and dried for 1 week at 45 °C before packing into tin capsules for elemental analysis. The amount of leachable DOC relative to the total C in from source soil and ash was computed by multiplying the concentration of DOC (mg/L) by the leaching volume (0.04 L), divided by the mass of dry material leached (4 g) and amount of C in the soil or ash (mg C/g dry mass) (eq 1)

$$\text{leachable DOC (mg/g)} = \frac{\text{DOC (mg/L)} \times \text{leaching volume (L)}}{\text{mass of mass of dry material (g)} \times \text{C content of dry solid (mg C/g)}} \quad (1)$$

This calculation reflects the proportion of soluble carbon relative to total carbon in the source material.[10]

2.4. Mixing Experiments with Ash and Aquatic DOM. Ash from three spatially separated areas of the CP and RF burn scar and corresponding leachates were selected for DOM mixing studies. Each of the three wildfire leachates were mixed on a per mass carbon (mg C) basis to ratios of 5, 10, 25, 50, and 75% wildfire DOM:aquatic isolate DOM, in three separate experiments. The aquatic DOM selected for these experiments was Upper Mississippi River Natural Organic Matter (MR NOM − Lot 1R110N) and is available for purchase from the International Humic Substances Society (IHSS). This aquatic isolate is similar in spectral characterization as Suwannee River isolates.[22] The three highly fluorescent ash leachates had contrasting $\phi_{f350} \geq 3.8\%$ relative to aquatic isolate Mississippi NOM ($\phi_{f350} = 1.25\%$) (Section 2.5). The stock solution of MR NOM was prepared in the same 0.01 $CaCl_2$ solution of Section 2.2 to keep the ionic matrix consistent for the mixing experiments. The stock MR NOM solution was diluted to a working concentration of 2.5 mg /L, verified by DOC analysis. Wildfire leachates were diluted to verified working concentrations of 1.5−2.5 mg C /L and mixed with MR NOM to solutions of 1 mg C/L achieving ratios of 5, 10, 25, 50, 75% mg ash: MR NOM. This final concentration of 1 ppm was selected to not exceed fluorescence detector limits with 75 or 100% highly fluorescent ash leachates. TOC concentrations of mixes were reverified after the experiments to ensure accurate computation of $SUVA_{254}$ and specific peak fluorescence.

2.5. Measurement and Calculation of Optical Indices. Filtered leachates of soils and ash were diluted to a range of 0.5−2.5 mg C/L to measure optical properties and not saturate the detector of the Fluoromax-4 fluorometer. Absorption spectra of wildfire leachates and surface waters were measured on an Agilent Cary 100 (Santa Clara, CA). Spectra were collected over 200−800 nm using 1 or 5 cm quartz cuvettes. Fluorescence EEMs were collected on a Jobin Yvon Fluoromax-4 over an excitation wavelength range of 240−450 nm over 10 nm increments and an emission range of 300−600 nm over 2 nm increments. All EEMs were blank corrected, corrected for primary and secondary inner-filter effects (IFE) and Raman scattering, and were Raman water normalized (MATLAB, Mathworks, MA).[23] More discussion about benchtop optical spectrum corrections is provided in Section S2, Ohno et al.,[24] Murphy et al.,[25,26] and Korak et al.[27] Absorbance and fluorescence spectra were measured in triplicate. The pH of all leachates and aquatic DOM mixtures were checked and remained between 6.9 and 7.4 via dilution $CaCl_2$ buffer, so optical shifts relative to unburned control leachates cannot be attributed to pH changes.[28]

The following optical metrics were computed for wildfire leachates: (i) absorbance metrics $SUVA_{254}$,[29] E_2:E_3, and slope ratio (S_R)[30] and (ii) fluorescence metrics of the humification index (HIX),[24] fluorescence index (FI),[31] biological index (BIX)[32] specific fluorescence peak and peak ratio assessments (normalized A, B, C, T and A:T, C:T),[13,33] and quantum yield.[34] Detailed definitions for the optical metrics of interest are provided in Table S2. The apparent fluorescence quantum yields (ϕ_f) for excitations of 300−450 nm were determined

https://doi.org/10.1021/acsestwater.3c00017
ACS EST Water 2023, 3, 2199−2209

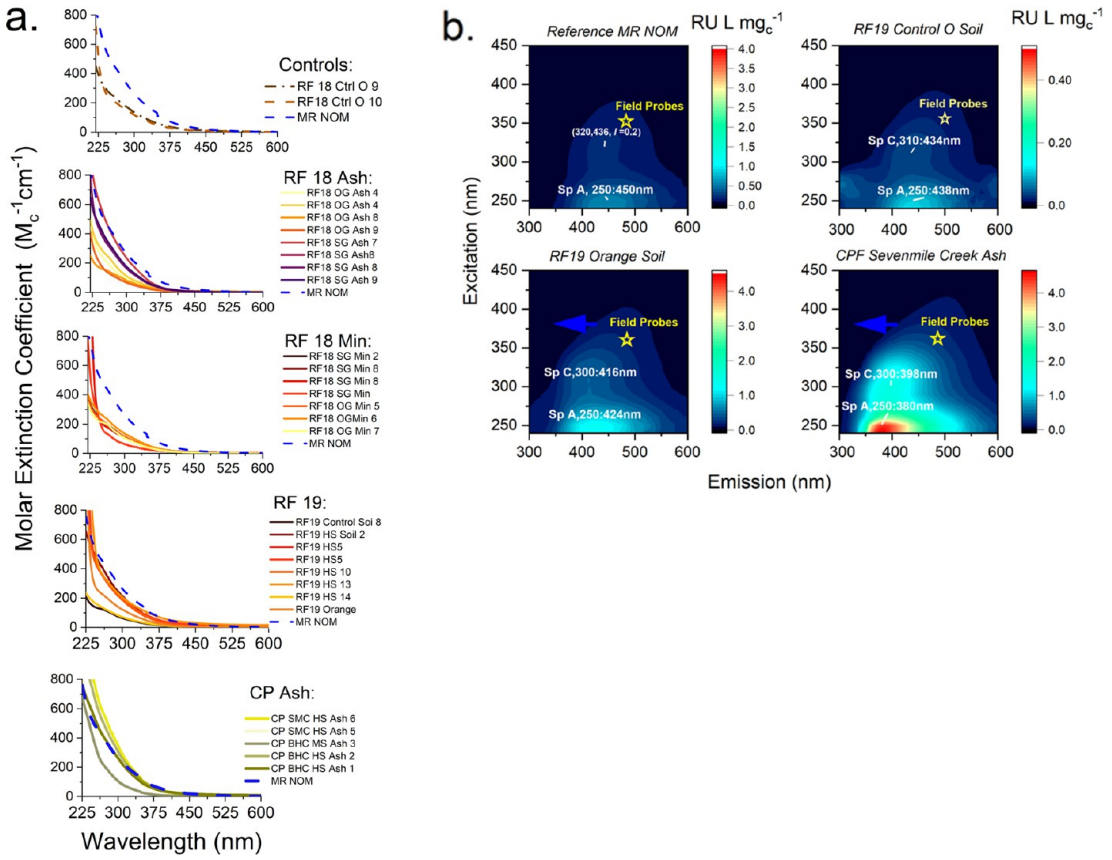

Figure 2. (a) Molar extinction coefficients or absorptivity of wildfire or reference soil leachates (M^{-1} cm^{-1}). (b) Fluorescence excitation−emission matrices (EEMs) of Mississippi NOM (MRNOM), unburned control soil leachate from outside the Ryan Fire, sampled 2019 (RF19), RF19 orange soil leachate, and Cameron Peak Sevenmile Creek ash from a high-severity area (CP SVN High Ash). Specific peak C and A locations are labeled Sp A/C. EEMs are presented in normalized water Raman Units (RU L mg C^{-1}) and scales are adjusted to EEM intensity. Blue arrows indicate EEM emission peaks that are blue-shifted relative to controls or isolates. Yellow star (★) indicates the region targeted by common commercial surface water or field probes (365 ± 5 nm:480 ± 40) (additional discussion in Section S2).

relative to quinine sulfate (QS) in 0.1 N sulfuric acid standard, as reported in McKay et al.[15] and Velapoldi.[35] Past experiments indicate excitation wavelengths <330 nm are subject to instrumental biases for the Fluoromax F4. This results in slightly inflated quantum yields at <330 nm.[15] Quantum yields were computed in MATLAB following previously described methods.[22,36] Results for 300−450 nm are reported in Figure S2. Fluorescence quantum yield at 350 nm was used for statistical comparisons and regressions as this value is not subject to instrumental biases and is the excitation maxima of quinine sulfate fluorescence.

2.6. Stream Sampling in the Cameron Peak Fire Burn Scar. The Cache Le Poudre (CLP) watershed is 4960 km^2 and ∼20% of this watershed forest was burned by the Cameron Peak fire. Combined, the Cameron Peak Fire and the 2012 High Park Fire burned more than 60% of the forested portion of the CLP watershed. To validate the optical metrics measured on wildfire ash and constrain the ranges used in our ash mixing experiments (Section 2.4) we evaluated surface water grab samples. Twenty samples were collected during nonstorm flow conditions from burned and unburned tributaries, as well as the main stem of the Cache la Poudre River in summer 2021. Another 12 samples were collected immediately following intense rainstorms (precipitation >5 cm/h) that generated "blackwater" events consisting of mobilized ash and sediment. Surface water samples were collected combusted 500 mL amber borosilicate glass containers and transported on ice to CU Boulder laboratories. Samples were filtered with pre-rinsed 0.7 um Whatman glass fiber filters into combusted 120 mL amber glass bottles within 12 h of collection. Filtered surface waters were stored refrigerated (4 °C) and in the dark for up to 2 weeks before analysis. DOC, absorbance scans, and EEMs were collected using the same equipment and procedures described above.

2.7. Statistics. Differences in physiochemical properties of pH and leachable DOC (Section 2.3) were tested between ash and burned and unburned mineral soils using one-way ANOVA with a post hoc Tukey comparison (Origin Lab Pro 2019, Northampton, MA). Optical metric differences for wildfire leachates were computed in pairwise comparisons via one-tailed Student *t*-tests with a null hypothesis of no difference between means. Materials were compared for old-growth and second-growth forests, reported burn severities, and ash/burned soil areas were resampled after snow and rainfall events (Tables S4 and S5 and Figure S3). Optical metrics were tested to differentiate leachates across different fire events, forest ages, impacted mineral soils versus ashes, burn severity, and time since the fire (Figure S3). The complete list of paired comparison is provided in Table S4. All tests included a comparison of optical properties for $n \geq 3$ spatial replicates per category. The significance of ANOVA and pairwise comparisons was set to $p < 0.05$ level. Linear

https://doi.org/10.1021/acsestwater.3c00017
ACS EST Water 2023, 3, 2199−2209

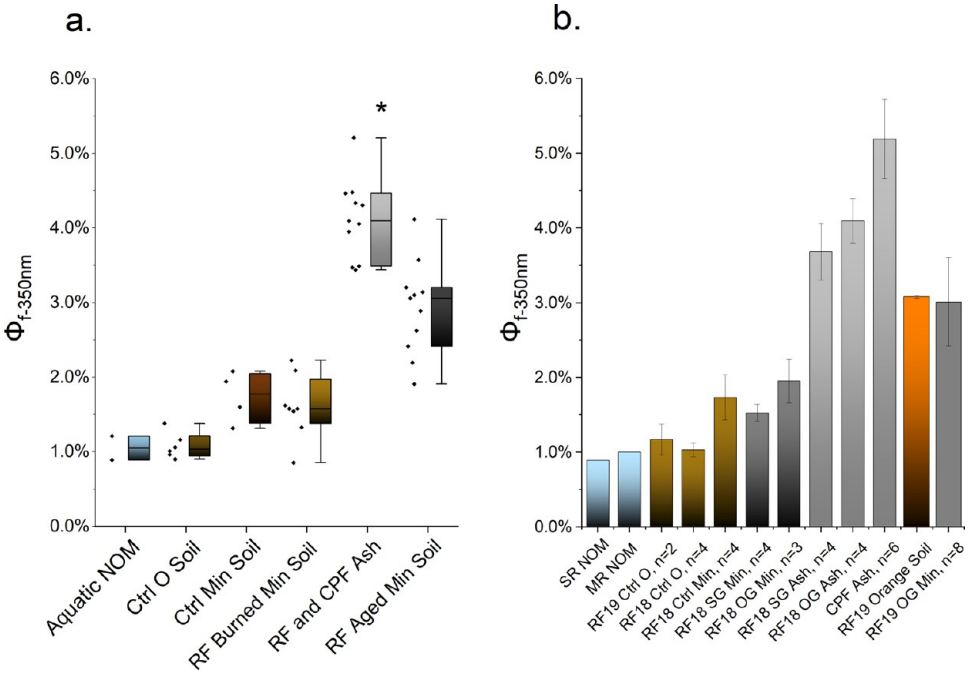

Figure 3. Fluorescence quantum yield at ex:350 nm ($\phi_{f\text{-}350nm}$) of leachates categorized by (a) aquatic NOM, control soils, mineral soils from RF18, high-severity ash and topsoil from RF18 and CP20, and 1 year later of RF19. The means of one or more levels were significantly different ($^*p < 0.05$) by a one-way ANOVA and *t*-tests. (b) Further details of wildfire leachate $\phi_{f\text{-}350nm}$ by wildfire setting. Box and bar colors denote either aquatic NOM (blue) or general colors of solid materials (Table S1).

regressions of optical indices as a function of ash leachate increases were computed for mixing experiments and the coefficient of determination, standard error of slope, and intercept were determined. Slope significance was set at $p < 0.05$. Stream samples (n = 31 total) were divided into three categories of: (i) burned tributaries or main Cache Le Poudre (CLP) river samples receiving drainage from all or a combination of burned and unburned CLP watershed area during normal or low flow conditions (n = 14), (ii) the same sites sampled during high-flow or poststorm conditions (n = 11), and (iii) reference tributary samples draining area entirely outside the CPF burnscar drainage, but still within the greater CLP watershed (n = 6) (Section S4 and Figure S4). Significant differences in DOM optical properties from these three categories were also compared via one-way ANOVA tests with a post hoc Tukey comparison of mean differences.

3. RESULTS AND DISCUSSION

3.1. Physical Characteristics of Source Material and Properties of Bulk Optical Spectrum. Ash and burned soils exhibited a wide range of pH, C:N ratios, and colors (Tables S1 and S2). The pH of unburned soil DOM was 6.1 ± 0.9 (n = 10), 6.5 ± 1.1 (n = 8) in burned mineral soil DOM, and elevated to 8.2 ± 0.6 (n = 6) ash leachate DOM (Figure S1). DOC was also lower for ash leachates than unburned soils and burned mineral soils (Figure S1). The %C of soils and ash ranged from 0.6 to 30.4% overall and was lowest in the orange, burned, weathered mineral soil collected post rain and snow events. The greatest %C was observed for the unburned organic layer soil collected outside the Ryan Fire burn scar. C:N ratios were greatest for unburned mineral soils collected outside the burn scar (63.7) and lowest for the orange, weathered mineral soil (16.4). Further details are provided in Section S1. The changes in source material C content, increased pH, and decreased DOC of the wildfire DOM are consistent with the production of $CaCO_3$, inorganic hydroxides, and the release of CO_2 that occurs during combustion.[17] All ashes and mineral soils generated enough DOC necessary for optical spectroscopy (Figure S1).

The absorbance and fluorescence intensities of wildfire-impacted DOM leachates were elevated or shifted toward the UV regions relative to an aquatic isolate and unburned soil leachates (Figure 2a). Fluorescence maxima of wildfire leachates were also blue-shifted relative to unburned soil leachate (Figure 2b and Supporting Information Datafile). Fluorescence-specific peaks A and C were present but in different locations for aquatic DOM reference, unburned soil leachate, orange mineral soil leachate, and a high-severity gray ash leachate (Figure 2). These peaks are classically attributed to overlapping signals of humic and fulvic acid-like fluorescence in the UV and visible regions.[37,38] Peak A Mississippi NOM was located at an ex/em = 250:450 nm. In contrast, peak A in gray ash was shifted 70 nm toward the UV range (ex/em 250:380 nm). Carbon-normalized intensities were 7-fold greater for ash leachates than unburned soil leachates. Elevated and shifted peak A and C intensities have also been observed for laboratory-combusted soil leachates.[15] The leachates in our study also exhibited a wide range of $\phi_{f\text{-}350}$ or fluorescence efficiencies (0.89% in unburned O-horizon leachates to 5.2% in gray ash leachates; Figure 3). Others have reported ϕ_f values that increase with lower molecular weight DOM,[39] and after combustion.[15] The range of increased ϕ_f in ash or burned soil leachates >2% reflects the natural variability in wildfire-derived DOM (Figure 3b). Elevated $\phi_{f\text{-}350}$ could be explained by increases in soluble aromatic fluorophores and polar electron donating groups like carboxylic acids likely increase with combustion in the presence of oxygen. Such observations have been noted in the molecular study of combusted OM via FTICR-MS.[5,17,1,28] In summary, basic

https://doi.org/10.1021/acsestwater.3c00017
ACS EST Water 2023, 3, 2199−2209

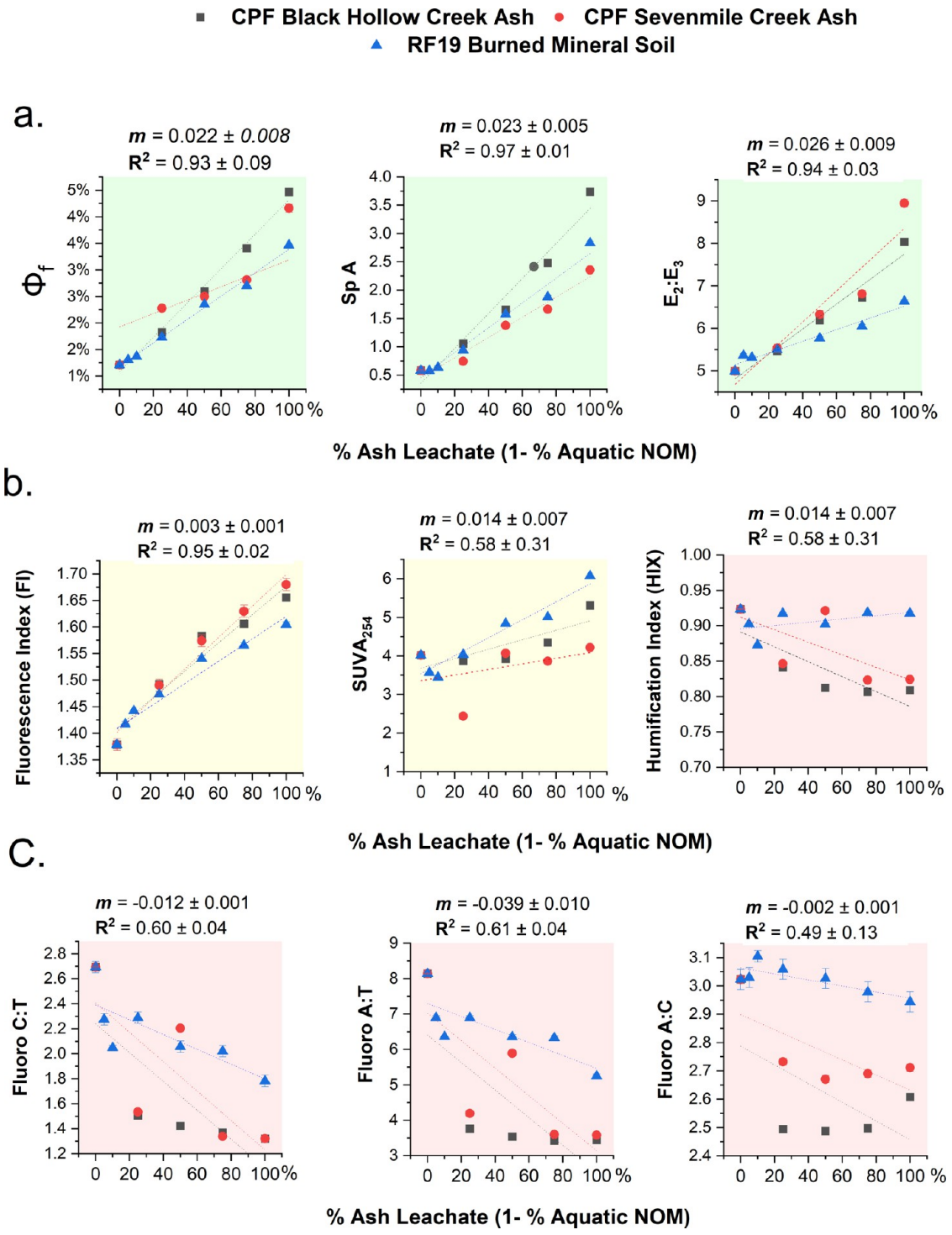

Figure 4. Linear response between optical fluorescence metrics and mixtures of ash and natural organic matter (NOM). The DOM leached from wildfire ash was mixed with Mississippi NOM in ratios of 0−100% ash (n = 3). Sample composites were Cameron Peak Fire (CP) Black Hollow Creek ash (gray square), CP Sevenmile Creek (SMC) Ash (red circle), and soil leachate from the Ryan Fire, 1-year post-fire (RF19 HS). (a) Plots are colored green for optical indices of slope (m) > 0.02, or R^2 (>0.93), (b) yellow for curvilinear response or m < 0.02, and (c) red for negative correlations as a function of increasing ash concentration.

appraisal of the bulk optical spectrum of wildfire-dissolved organic matter indicated that spectra are generally UV shifted and highly fluorescent, and therefore may not be successfully quantitated by conventional methods for unimpacted DOM.

Leachates from fresh, gray ash from areas with high-severity burning had the greatest average fluorescence efficiency ($\phi_{f\text{-}350}$ = 4.12 ± 0.53%) (n = 11, Figure 3a). $\phi_{f\text{-}350}$ of fresh ash leachates were 4 times greater than isolates MR NOM, Suwanee River NOM,[14] or unburned O horizon leachates that were 1.06 ± 0.2% (Figure 3a). Interestingly, $\phi_{f\text{-}350}$ of ash leachates was also significantly greater than burned mineral soil leachates collected 1 year after the Ryan Fire (n = 11, $\phi_{f\text{-}350}$ = 2.93 ± 0.62%, Figure 3). The decrease in $\phi_{f\text{-}350}$ with time since burning could indicate weathering or transport of surface ashes

https://doi.org/10.1021/acsestwater.3c00017
ACS EST Water 2023, 3, 2199−2209

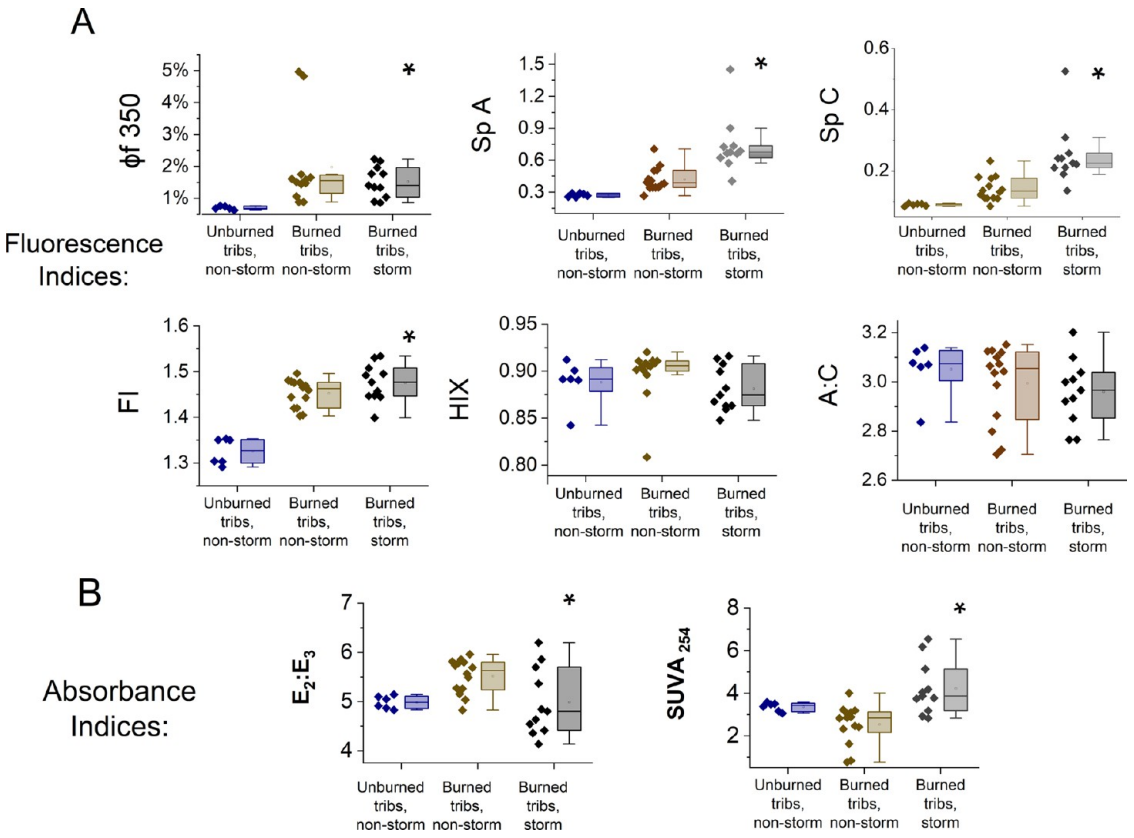

Figure 5. (A, B) Optical indices of filtered surface water DOM from burned and unburned tributaries of the Cache Le Poudre (CLP) watershed that was impacted by the Cameron Peak Fire, 2020. Samples (n = 32) were collected over 11 dates in unburned tributaries—normal flows (n = 5), burned tributaries—normal flows/nonstorm (n = 17), and burned tributaries—storm/high flows (n = 13).

with high $\phi_{f\text{-}350}$. In contrast, $\phi_{f\text{-}350}$ were similar in leachates from unburned and burned mineral soils, which indicates that this wildfire had limited impact on DOM released from the upper 10 cm of mineral soil. The soil and ash samples spanned a range of brown, black, gray, and reddish-orange color that was reflected in the $\phi_{f\text{-}350}$ of leached DOM; the light gray ash had the greatest $\phi_{f\text{-}350}$ (Figure 3a and Table S1). Implications of ash color in burn severity assessment and ash chemistry are further discussed in the Supporting Information. Overall, the significant range of $\phi_{f\text{-}350}$ across forest settings is consistent with previous research that shows a range of pH, colors, mineral content, and optical and molecular properties possible for wildfire materials.[14,15] This suggests $\phi_{f\text{-}350}$ could be further developed as a valuable technique to discern wildfire leachate variability on spatial, temporal, and severity scales.

3.2. Laboratory Study Of Optical Metrics for Wildfire DOM Differentiation. Studies report elevated FI, HIX, or $SUVA_{254}$ in waterways with post-wildfire inputs.[4,7] Limited research has tested which optical indices best correlate to wildfire-derived DOM increases in the presence of non-impacted, aquatic DOM however in controlled experiments. In mixing experiment analysis (Section 2.4), only a subset of the 12 optical metrics we tested had additive, linear increases in optical signal proportional to increasing concentrations of wildfire DOM. The UV fluorescence peak Sp A (ex/em ≈ 250:380), had the greatest positive linear response to increasing ash content; slopes were 3 times greater than for Sp C, B, or T (Figure S4). Conversely, there was essentially no fluorescence response in the high UV excitation and emission ranges associated with Sp B and Sp T across the range of these ash concentrations. For this reason, mixing experiment changes based on fluorescence peak ratio calculations of A:T and C:T were weak or negatively correlated (Figure 4c). The strong linear correlation coefficients of R^2 > 0.95 for Sp A and C mixing indicated additive property balance principles (Figure S4) and their potential for detecting wildfire-derived DOM mixtures. This analysis was computed for actual fluorescence maxima and not pre-set peak regions.[13] Computations on actual fluorescence peak maxima are more accurate in diverse applications because maxima can shift outside classically defined bounds first defined for marine samples.[19,23] Based on the slope and response range, Sp A is the best fluorescence peak surrogate for these ash samples and concentrations. However, Sp A typically occurs around ex ≈ 250 nm, which is more susceptible to IFE errors than Sp C at ex ≈ 320−360 nm, an issue further discussed in Section S2.[18] Thus, use of Sp A requires adequate IFE correction.[24,40]

Other optical metrics ϕ_{f350} and E_2:E_3 increased positively to ash concentration in NOM mixtures (Figure 4). Linear relationships for FI and $SUVA_{254}$ were weaker (m < 0.02) or curvilinear. Korak et al.[23] also reported a curvilinear response of FI in end-member mixing experiments of autochthonous Pony Lake Fulvic Acid PLFA with allochthonous Suwannee River Humic Acid (SRHA), which is because it is calculated as the ratio of em = 470/570 nm at ex = 370 nm. Wildfire Fluorescence Peak A maxima occurred on average at 412 ± 18 nm and Peak C maxima occurred at 409 ± 11 nm on average (n = 28, Supporting Information Datafile). Therefore, wildfire maxima were consistently UV-shifted away from 470 and 570 nm and FI is computed on long-wavelength maxima shoulders

https://doi.org/10.1021/acsestwater.3c00017
ACS EST Water 2023, 3, 2199−2209

with a tailing signal at 570 nm, resulting in curvilinear FI values.[23] HIX is computed as the ratio of area under em: 435−480 nm/em 300−345 nm. As ash EEMs UV-shift, the denominator of HIX increases and the signal in the visible region decreases, resulting in negative correlations of HIX with increasing ash concentrations (Figure 4b). $SUVA_{254}$ is another parameter that is widely utilized in drinking and wastewater monitoring that did not perform well in our study. $SUVA_{254}$ may have had a weaker R^2 than other parameters because it is computed based on highly variable DOC measurements (i.e., +∼2% difference among duplicate samples).[23]

3.3. Optical Properties of Surface Waters Draining from Burned Tributaries. DOM fluorescence indices ϕ_{f350}, Sp A, Sp C, and FI were significantly elevated in burned tributaries relative to unburned tributaries in both storm and nonstorm flows of the CLP watershed (Tukey post hoc tests, Figure S5). As with mixing experiments, HIX and peak ratio A:C (as well as A:T and C:T, Section 3.3) did not detect significant differences in optical properties for burned or unburned stream DOM. Absorbance metrics of E_2:E_3 and $SUVA_{254}$ were both significantly elevated for burned tributaries in nonstorm and storm conditions compared to unburned surface waters.

The range and elevation of optical indices were comparable from lab to surface water mixes (Figure 5 and Table S5). For example, average $SUVA_{254}$ measured in high/storm flows of burned tributaries was elevated to 4.2 ± 1.2 L/mg-m (n = 17) relative to unburned waters (3.4 ± 0.3 L/mg-m). Elevated levels were consistent with 50:50 mixes of Seven mile Creek or Black Hollow ash:aquatic NOM = 4.0 ± 0.2 L/mg-m. ϕ_{f350} of DOM from nonstorm burned tributaries reached values as high as 4.8%, which is in range with ϕ_{f350} of > 90% ash in controlled mixes. We cannot extrapolate lab results to actual ash concentrations in surface waters because we do not know the complex hydrology of field conditions at the time of sampling. Rather, laboratory combinations >25% ash leachate broadly suggest there were consistent and significant inputs of ash and burned soil that elevated optical metrics in the summer sampling campaign, post-fire. Like ash and burned soil that was leached in a laboratory setting, EEM peak A and C maxima of burned watershed tributaries were also 20−30 nm UV-shifted relative to unburned EEMs (Table S5). Therefore, commercial surface water or field probes set to standard ex/em couple of 365 ± 5/480 ± 40 nm would have reduced sensitivity or miss wildfire DOM's peak fluorescence at ex/em of 319 ± 3/421 ± 6 nm.

3.4. Implications of Monitoring Streams in Burned Watersheds. Optical properties of leached ash, soils, and wildfire-impacted surface waters reflect significant differences between pyrogenically influenced DOM and DOM from unburned soils and streams. This work suggests optical sensors could be developed to better target the unique optical properties of ash *in situ*. For benchtop analyses, optical spectra can be analyzed for summative metrics that are the strongest tracers for wildfire effects. We found that ϕ_{f350}, Sp A, and E_2:E_3 were the best indices to characterize and quantify wildfire-affected soil and ash leachates (Figure 4). However, we applied IFE corrections to all EEMs before metrics were computed, which would complicate the use of currently available fluorescence-based probes. Other challenges exist. For example, the fluorescence peak maxima measured for wildfire leachates and surface waters are outside of the range measured by commercial water quality probes that currently target narrow, preset wavelength couples (i.e., 365 ± 5:480 ± 40 nm); this is further discussed in Section S2.[38,41] In our study, the fluorescence peak C of high severity CP ash leachate equaled ex:em 300:398 nm (Figure 2b) which would not have been measured by conventional surface water probes or algorithm-based optical indices. Further, the preset wavelength regions can cause issues when mixing DOM from contrasting origins. For example, Korak et al.[27] demonstrated that optical metrics do not reflect property balance principles when computed on the slope or shoulders of fluorescence maxima, rather than peak values. Misaligned optical quantification on slopes of wildfire fluorescence signals could reduce detection or differentiation capabilities.[18,19]

Future probes developed to measure ϕ_{f350} and Sp A would require *post hoc* IFE fluorescence corrections, in-line IFE corrections, or tests to determine the degree of impact of reporting uncorrected data since current probes do not automate IFE corrections[27,40] This topic is further discussed in Section S2. Neither FI nor HIX performed well in mixing experiments, environmental leachate comparisons, or surface water sample differentiation (Figures 4, 5, and S3) because they do not accommodate the blue-shifted maxima of wildfire-derived DOM. Peak ratio computations of A:C and A:T also did not perform well for wildfire comparisons, unlike what was been demonstrated for wastewater effluent experiments.[18]

In contrast to the fluorescence metrics, the absorbance-based metric E_2:E_3 performed well in mixing experiments and was elevated in burned CLP tributary. This metric is not impacted by IFE or DOC measurement error (Table S3). E_2:E_3 is only based on two absorbance wavelengths (250 nm and 364 nm) and may be more feasible for use in probes than $SUVA_{254}$ (Section S2). However, UV region absorbance-based metrics are susceptible to interference from high dissolved iron (III) concentrations (>0.5 ppm). Iron (III) corrections have been developed for $SUVA_{254}$[42] and limited work has examined corrections for E_2:E_3. Iron interference could limit the utility of E_2:E_3 in areas with iron-rich lithology.[43] In such areas, a corrected $SUVA_{254}$ measurements with Fe(III) corrections could be more appropriate than E_2:E_3.

A limitation of this study is that we did not evaluate all spectral analysis techniques such as Fluorescence Regional Integration (FRI) or Parallel Factor Analysis (PARAFAC),[44] which also have recognized limitations.[45] FRI is constrained by the rigid boundaries definitions. PARAFAC is a robust and flexible EEM modeling tool with a complimentary online database for models (https://openfluor.lablicate.com/),[46] but requires full, corrected spectrums, sufficient spectrums to model together (i.e., ∼15 for statistical requirements). PARAFAC models may require prior experience in order to avoid incorrectly ascribing model components.[25,47] In contrast, application of a focused set of application-specific optical metrics such as ϕ_{f}, peak C, and E_2:E_3 would require fewer steps and less user training for use in routine monitoring in environment studies or water treatment applications.[7,9] The surface water samples included herein were filtered and measured on bench-top spectrophotometers. Therefore, additional considerations or corrections of turbidity, particulate matter and temperature on different optical metrics will need to be explored to develop *in situ* optical probes for wildfire-impacted waters. Recent progress with these corrections is discussed in Section S2.

3.5. Future Research Needs. Our work demonstrates that certain optical indices have value as proxies for detecting

https://doi.org/10.1021/acsestwater.3c00017
ACS EST Water 2023, 3, 2199−2209

wildfire ash inputs in the aquatic DOM of wildfire-affected coniferous headwaters, but further study is needed to assess the applicability of this approach in other ecosystem types such as prairie, deciduous forest, and other climates.[48] Follow-up could attempt to directly explain ϕ_{fi} peak C, E_2:E_3 surface water variability due to seasonal and storm event patterns with a detailed hydrological study.[4,7,49] The fundamental mechanisms that link wildfire DOM quality and combustion conditions (i.e., fuel, temperature, and oxygen) remain elusive and inconsistent between laboratory and field conditions.[11,15] For example, none of our field samples demonstrated the elevated optical response (ϕ_{f370} > 8%) of DOM that has been documented during laboratory heating studies.[11,15] Experimental pyrocosms composed of forest debris, soil, and combusted outdoors that may help bridge the gap between laboratory and wildfire studies to advance a general understanding of post-fire DOM changes. Qualitative interpretations of many optical indices also may classically refer to microbial degradation or biogeochemical shifts that may not be appropriate for evaluating changes associated with wildfires. Future work that integrates the convenience of optical indices with high resolution of molecular methods (i.e., FTICR-MS, ^{13}C NMR[50]) has potential to improve mechanistic understanding of ash chemistry and water quality impacts.

4. CONCLUSIONS

Although optical metrics were originally developed to characterize DOM variability in undisturbed freshwater and marine ecosystems, we found that only a subset of them also have the potential for detecting shifts in DOM character in ash leachates and burned watersheds. Specifically, we found that ϕ_{fi} specific peak C, and E_2:E_3 differentiated DOM from ash, burned soil leachates, and surface waters from burned watersheds across a wide range of conditions. Conversely, other common optical metrics (FI, HIX, A:T, C:T, and A:C) were poor indicators of dissolved ash quality and quantity due to the UV-shifted nature of wildfire DOM. Using a combination of the metrics (e.g., ϕ_{fi}, fluorescence peak A or C, E_2:E_3, and $SUVA_{254}$ where Fe (III) concentrations are low) can help researchers overcome the methodological limitations of optical metrics to improve the detection of trace ash concentrations in surface water. This work identifies which optical measures have the greatest potential for detecting the unique DOM spectra of ash and burned soils and should help inform the development of *in situ* measurement approaches and tools for monitoring wildfire impacts.

■ ASSOCIATED CONTENT

Supporting Information

The Supporting Information is available free of charge at https://pubs.acs.org/doi/10.1021/acsestwater.3c00017.

Optical metrics for 40 samples (XLSX)

Photographs, pH data, and leachable carbon characterization of ash and soils; a description of fluorescence probes; corrections; table of metric definitions; fluorescence quantum yield calculation and range results; and pairwise comparisons of optical metrics to differentiate wildfire leachates across forest settings (PDF)

■ AUTHOR INFORMATION

Corresponding Authors

Sarah J. Fischer − *Department of Civil, Environmental and Architectural Engineering, University of Colorado Boulder, Boulder, Colorado 80309, United States; Environmental Engineering Program, University of Colorado Boulder, Boulder, Colorado 80309, United States;* Present Address: Department of Civil and Environmental Engineering, University of Missouri, Columbia, Missouri 65201, United States; orcid.org/0000-0001-5460-4174; Email: sjfischer@missouri.edu

Fernando L. Rosario-Ortiz − *Department of Civil, Environmental and Architectural Engineering, University of Colorado Boulder, Boulder, Colorado 80309, United States; Environmental Engineering Program, University of Colorado Boulder, Boulder, Colorado 80309, United States;* orcid.org/0000-0002-3311-9089; Email: fernando.rosario@colorado.edu

Authors

Timothy S. Fegel − *Rocky Mountain Research Station, US Forest Service, United States Department of Agriculture, Fort Collins, Colorado 80526, United States*

Paul J. Wilkerson − *Environmental Engineering Program, University of Colorado Boulder, Boulder, Colorado 80309, United States*

Leah Rivera − *Environmental Engineering Program, University of Colorado Boulder, Boulder, Colorado 80309, United States*

Charles C. Rhoades − *Rocky Mountain Research Station, US Forest Service, United States Department of Agriculture, Fort Collins, Colorado 80526, United States*

Complete contact information is available at: https://pubs.acs.org/10.1021/acsestwater.3c00017

Author Contributions

CRediT: **Sarah Fischer** conceptualization (equal), data curation (lead), formal analysis (equal), investigation (lead), methodology (lead), validation (lead), visualization (lead), writing-original draft (lead), writing-review & editing (supporting); **Tim Fegel** conceptualization (supporting), data curation (supporting), investigation (supporting), methodology (supporting), resources (supporting), visualization (supporting), writing-review & editing (supporting); **Paul J. Wilkerson** data curation (supporting), investigation (supporting), methodology (supporting), validation (supporting), writing-review & editing (supporting); **Leah Rivera** data curation (supporting), formal analysis (supporting), investigation (supporting), software (supporting); **Charles C. Rhoades** conceptualization (equal), data curation (supporting), formal analysis (supporting), investigation (lead), project administration (equal), resources (supporting), validation (supporting), writing-original draft (supporting), writing-review & editing (equal); **Fernando L. Rosario-Ortiz** conceptualization (equal), formal analysis (supporting), funding acquisition (lead), investigation (supporting), project administration (lead), resources (supporting), supervision (lead), writing-review & editing (equal).

Notes

The authors declare no competing financial interest.

https://doi.org/10.1021/acsestwater.3c00017
ACS EST Water 2023, 3, 2199−2209

■ ACKNOWLEDGMENTS

Thanks go to Dr. James McCutchen for his thorough and helpful CHN Analysis conducted at the Center for Environmental Systems Analysis, CU Boulder and to instrument and lab managers Stefan Peterson and Dorothy Noble for their analytical support at CU Boulder. L.R. was supported by the CU Boulder Undergraduate Research Opportunity (UROP) summer scholarship and the Discovery Learning Apprenticeship (DLA) program within the Civil and Environmental Engineering department, CU Boulder. Thanks also go to Taylor Motley for her efforts in watershed sampling and processing optical data of stream samples and to Mackenzie Bowden for providing details about stream sampling. Lastly, thanks go to the two anonymous reviewers whose feedback enhanced this manuscript.

■ REFERENCES

(1) (a) Abatzoglou, J. T.; Williams, A. P. Impact of anthropogenic climate change on wildfire across western US forests. *Proc. Natl. Acad. Sci. U.S.A.* **2016**, *113*, 11770−11775. (b) Radeloff, V. C.; Helmers, D. P.; Kramer, H. A.; Mockrin, M. H.; Alexandre, P. M.; Bar-Massada, A.; Butsic, V.; Hawbaker, T. J.; Martinuzzi, S.; Syphard, A. D.; Stewart, S. I. Rapid growth of the US wildland-urban interface raises wildfire risk. *Proc. Natl. Acad. Sci. U.S.A.* **2018**, *115*, 3314−3319.

(2) (a) Parks, S. A.; Miller, C.; Parisien, M.-A.; Holsinger, L. M.; Dobrowski, S. Z.; Abatzoglou, J. Wildland fire deficit and surplus in the western United States, 1984−2012. *Ecosphere* **2015**, *6*, No. art275. (b) Syphard, A. D.; Radeloff, V. C.; Keeley, J. E.; Hawbaker, T. J.; Clayton, M. K.; Stewart, S. I.; Hammer, R. B. Human influence on California fire regimes. *Ecol. Appl.* **2007**, *17*, 1388−1402.

(3) Emelko, M. B.; Silins, U.; Bladon, K. D.; Stone, M. Implications of land disturbance on drinking water treatability in a changing climate: Demonstrating the need for "source water supply and protection" strategies. *Water Res.* **2011**, *45*, 461−472.

(4) Hohner, A. K.; Rhoades, C. C.; Wilkerson, P.; Rosario-Ortiz, F. L. Wildfires Alter Forest Watersheds and Threaten Drinking Water Quality. *Acc. Chem. Res.* **2019**, *52*, 1234−1244.

(5) Mack, E.; Lilja, R.; Claggett, S.; Sun, G.; Caldwell, P. *Forests to Faucets 2.0: Connecting Forests, Water, and Communities* U.S. Department of Agriculture, Forest Service: Washington, DC; 2022.

(6) (a) Santín, C.; Stefan; Xosé; Chafer, C. J. Quantity, composition and water contamination potential of ash produced under different wildfire severities. *Environ. Res.* **2015**, *142*, 297−308. (b) Smith, H. G.; Sheridan, G. J.; Lane, P. N. J.; Nyman, P.; Haydon, S. Wildfire effects on water quality in forest catchments: A review with implications for water supply. *J. Hydrol.* **2011**, *396*, 170−192.

(7) Uzun, H.; Dahlgren, R. A.; Olivares, C.; Erdem, C. U.; Karanfil, T.; Chow, A. T. Two years of post-wildfire impacts on dissolved organic matter, nitrogen, and precursors of disinfection by-products in California stream waters. *Water Res.* **2020**, *181*, No. 115891.

(8) Becker, W. C.; Hohner, A.; Rosario-Ortiz, F.; Dewolfe, J. Preparing for Wildfires and Extreme Weather: Plant Design and Operation Recommendations. *J. Am. Water Works Assoc.* **2018**, *110*, 32−40.

(9) Hohner, A. K.; Terry, L. G.; Townsend, E. B.; Summers, R. S.; Rosario-Ortiz, F. L. Water treatment process evaluation of wildfire-affected sediment leachates. *Environ. Sci.: Water Res. Technol.* **2017**, *3*, 352−365.

(10) Wilkerson, P. J.; Rosario-Ortiz, F. L. Impact of simulated wildfire on disinfection byproduct formation potential. *AWWA Water Sci.* **2021**, *3*, No. e1217.

(11) Wang, J.-J.; Dahlgren, R. A.; Chow, A. T. Controlled Burning of Forest Detritus Altering Spectroscopic Characteristics and Chlorine Reactivity of Dissolved Organic Matter: Effects of Temperature and Oxygen Availability. *Environ. Sci. Technol.* **2015**, *49*, 14019−14027.

(12) Wang, J.-J.; Dahlgren, R. A.; Erşan, M. S.; Karanfil, T.; Chow, A. T. Wildfire Altering Terrestrial Precursors of Disinfection Byproducts in Forest Detritus. *Environ. Sci. Technol.* **2015**, *49*, 5921−5929.

(13) Gabor, R. S.; Baker, A.; McKnight, D. M.; Miller, M. P.Fluorescence Indices and Their Interpretation. In *Aquatic Organic Matter Fluorescence*; Cambridge University Press, 2014; p 303.

(14) Cawley, K. M.; Hohner, A. K.; Podgorski, D. C.; Cooper, W. T.; Korak, J. A.; Rosario-Ortiz, F. L. Molecular and Spectroscopic Characterization of Water Extractable Organic Matter from Thermally Altered Soils Reveal Insight into Disinfection Byproduct Precursors. *Environ. Sci. Technol.* **2017**, *51*, 771−779.

(15) McKay, G.; Hohner, A. K.; Rosario-Ortiz, F. L. Use of optical properties for evaluating the presence of pyrogenic organic matter in thermally altered soil leachates. *Environ. Sci.: Processes Impacts* **2020**, *22*, 981−992.

(16) (a) Aiken, G. R.Fluorescence and Dissolved Organic Matter: A Chemist's Perspective. In *Aquatic Organic Matter Fluorescence*; Cambridge University Press, 2014; pp 35−74. (b) Cawley, K. M.; Hohner, A. K.; McKee, G. A.; Borch, T.; Omur-Ozbek, P.; Oropeza, J.; Rosario-Ortiz, F. L. Characterization and spatial distribution of particulate and soluble carbon and nitrogen from wildfire-impacted sediments. *J. Soils Sediments* **2018**, *18*, 1314−1326.

(17) Bodí, M. B.; Martin, D. A.; Balfour, V. N.; Santín, C.; Doerr, S. H.; Pereira, P.; Cerdà, A.; Mataix-Solera, J. Wildland fire ash: Production, composition and eco-hydro-geomorphic effects. *Earth-Sci. Rev.* **2014**, *130*, 103−127.

(18) Ulliman, S. L.; Korak, J. A.; Linden, K. G.; Rosario-Ortiz, F. L. Methodology for selection of optical parameters as wastewater effluent organic matter surrogates. *Water Res.* **2020**, *170*, No. 115321.

(19) Fischer, S. J.; Gonsior, M.; Chorover, J.; Powers, L. C.; Hamilton, A.; Ramirez, M.; Torrents, A. Biosolids leachate variability, stabilization surrogates, and optical metric selection. *Environ. Sci.: Water Res. Technol.* **2022**, *8*, 657−670.

(20) Parsons, A.; Robichaud, P. R.; Lewis, S. A.; Napper, C.; Clark, J. T. *Field Guide for Mapping Post-Fire Soil Burn Severity*, General Technical Report RMRS-GTR-243US, Department of Agriculture, Forest Service, Rocky Mountain Research Station; 2010.

(21) Gabor, R. S.; Burns, M. A.; Lee, R. H.; Elg, J. B.; Kemper, C. J.; Barnard, H. R.; McKnight, D. M. Influence of Leaching Solution and Catchment Location on the Fluorescence of Water-Soluble Organic Matter. *Environ. Sci. Technol.* **2015**, *49*, 4425−4432.

(22) McKay, G.; Korak, J. A.; Erickson, P. R.; Latch, D. E.; McNeill, K.; Rosario-Ortiz, F. L. The Case Against Charge Transfer Interactions in Dissolved Organic Matter Photophysics. *Environ. Sci. Technol.* **2018**, *52*, 406−414.

(23) Korak, J. A.; Dotson, A. D.; Summers, R. S.; Rosario-Ortiz, F. L. Critical analysis of commonly used fluorescence metrics to characterize dissolved organic matter. *Water Res.* **2014**, *49*, 327−338.

(24) Ohno, T. Fluorescence inner-filtering correction for determining the humification index of dissolved organic matter. *Environ. Sci. Technol.* **2002**, *36*, 742−746.

(25) Murphy, K. R.; Butler, K. D.; Spencer, R. G. M.; Stedmon, C. A.; Boehme, J. R.; Aiken, G. R. Measurement of Dissolved Organic Matter Fluorescence in Aquatic Environments: An Interlaboratory Comparison. *Environ. Sci. Technol.* **2010**, *44*, 9405−9412.

(26) Murphy, K. R.; Stedmon, C. A.; Graeber, D.; Bro, R. Fluorescence spectroscopy and multi-way techniques. PARAFAC. *Anal. Methods* **2013**, *5*, 6557−6566.

(27) Korak, J. A.; Rosario-Ortiz, F.; Summers, R. S. Fluorescence Characterization of Humic Substance Coagulation: Application of New Tools to an Old Process. In *Advances in the Physicochemical Characterization of Dissolved Organic Matter: Impact on Natural and Engineered Systems*; Rosario-Ortiz, F., Ed.; ACS, 2014; pp 281−300.

(28) Aiken, G. R.Fluorescence and Dissolved Organic Matter: A Chemist's Perspective. In *Aquatic Organic Matter Fluorescence*; Cambridge University Press, 2014; pp 35−75.

(29) Weishaar, J. L.; Aiken, G. R.; Bergamaschi, B. A.; Fram, M. S.; Fujii, R.; Mopper, K. Evaluation of specific ultraviolet absorbance as

https://doi.org/10.1021/acsestwater.3c00017
ACS EST Water 2023, 3, 2199−2209

an indicator of the chemical composition and reactivity of dissolved organic carbon. *Environ. Sci. Technol.* **2003**, *37*, 4702−4708.
(30) Helms, J. R.; Stubbins, A.; Ritchie, J. D.; Minor, E. C.; Kieber, D. J.; Mopper, K. Absorption spectral slopes and slope ratios as indicators of molecular weight, source, and photobleaching of chromophoric dissolved organic matter. *Limnol. Oceanogr.* **2008**, *53*, 955−969.
(31) Cory, R. M.; McKnight, D. M. Fluorescence spectroscopy reveals ubiquitous presence of oxidized and reduced quinones in dissolved organic matter. *Environ. Sci. Technol.* **2005**, *39*, 8142−8149.
(32) (a) Huguet, A.; Vacher, L.; Relexans, S.; Saubusse, S.; Froidefond, J. M.; Parlanti, E. Properties of fluorescent dissolved organic matter in the Gironde Estuary. *Org. Geochem.* **2009**, *40*, 706−719. (b) Parlanti, E.; Worz, K.; Geoffroy, L.; Lamotte, M. Dissolved organic matter fluorescence spectroscopy as a tool to estimate biological activity in a coastal zone submitted to anthropogenic inputs. *Org. Geochem.* **2000**, *31*, 1765−1781.
(33) Hansen, A. M.; Tamara, E. C.; Pellerin, B. A.; Fleck, J. A.; Downing, B. D.; Bergamaschi, B. A. Optical properties of dissolved organic matter (DOM): Effects of biological and photolytic degradation. *Limnol. Oceanogr.* **2016**, *61*, 1015−1032.
(34) McKay, G.; Huang, W.; Romera-Castillo, C.; Crouch, J. E.; Rosario-Ortiz, F. L.; Jaffé, R. Predicting Reactive Intermediate Quantum Yields from Dissolved Organic Matter Photolysis Using Optical Properties and Antioxidant Capacity. *Environ. Sci. Technol.* **2017**, *51*, 5404−5413.
(35) Velapoldi, R. A.; Mielenz, K. D. *A Fluorescence Standard Reference Material: Quinine Sulfate Dihydrate*; US Department of Commerce, National Bureau of Standards, 1980; pp 260−264.
(36) Mckay, G.; Korak, J. A.; Rosario-Ortiz, F. L. Temperature Dependence of Dissolved Organic Matter Fluorescence. *Environ. Sci. Technol.* **2018**, *52*, 9022−9032.
(37) Korak, J. A.; Rosario-Ortiz, F. L.; Summers, R. S. Fluorescence Characterization of Humic Substance Coagulation: Application of New Tools to an Old Process. In *Advances in the Physicochemical Characterization of Dissolved Organic Matter: Impact on Natural and Engineered Systems*; RosarioOrtiz, F., Ed.; ACS, 2014; Vol. *1160*, pp 281−300.
(38) Chen, W.; Westerhoff, P.; Leenheer, J. A.; Booksh, K. Fluorescence excitation-emission matrix regional integration to quantify spectra for dissolved organic matter. *Environ. Sci. Technol.* **2003**, *37*, 5701−5710.
(39) Hanson, B.; Wünsch, U.; Buckley, S.; Fischer, S.; Leresche, F.; Murphy, K.; D'Andrilli, J.; Rosario-Ortiz, F. L. DOM Molecular Weight Fractionation and Fluorescence Quantum Yield Assessment Using a Coupled In-Line SEC Optical Property System. *ACS ES&T Water* **2022**, *2*, 2491−2501.
(40) Tucker, S. A.; Amszi, V. L.; William, E.; Acree, J. Primary and Secondary Inner Filtering: Effect of K2Cr207 on Fluorescence Emission Intensities of Quinine Sulfate. *J. Chem. Educ.* **1992**, *69*, No. A8.
(41) Shutova, Y.; Baker, A.; Bridgeman, J.; Henderson, R. K. On-line monitoring of organic matter concentrations and character in drinking water treatment systems using fluorescence spectroscopy. *Environ. Sci.: Water Res. Technol.* **2016**, *2*, 749−760.
(42) Poulin, B. A.; Ryan, J. N.; Aiken, G. R. Effects of Iron on Optical Properties of Dissolved Organic Matter. *Environ. Sci. Technol.* **2014**, *48*, 10098−10106.
(43) Stirchak, L. T.; Moor, K. J.; McNeill, K.; Donaldson, D. J. Differences in photochemistry between seawater and freshwater for two natural organic matter samples. *Environ. Sci.: Processes Impacts* **2019**, *21*, 28−39.
(44) Batista-Andrade, J. A.; Diaz, E.; Iglesias Vega, D.; Hain, E.; Rose, M. R.; Blaney, L. Spatiotemporal analysis of fluorescent dissolved organic matter to identify the impacts of failing sewer infrastructure in urban streams. *Water Res.* **2023**, *229*, No. 119521.
(45) Rosario-Ortiz, F. L.; Korak, J. A. Oversimplification of Dissolved Organic Matter Fluorescence Analysis: Potential Pitfalls of Current Methods. *Environ. Sci. Technol.* **2017**, *51*, 759−761.
(46) Murphy, K. R.; Stedmon, C. A.; Wenig, P.; Bro, R. OpenFluor−an online spectral library of auto-fluorescence by organic compounds in the environment. *Anal. Methods* **2014**, *6*, 658−661.
(47) Mostofa, K. M. G.; Jie, Y.; Sakugawa, H.; Liu, C.-Q. Equal Treatment of Different EEM Data on PARAFAC Modeling Produces Artifact Fluorescent Components That Have Misleading Biogeochemical Consequences. *Environ. Sci. Technol.* **2019**, *53*, 561−563.
(48) (a) Jaffé, R.; Ding, Y.; Niggemann, J.; Vahatalo, A. V.; Stubbins, A.; Spencer, R. G. M.; Campbell, J.; Dittmar, T. Global Charcoal Mobilization from Soils via Dissolution and Riverine Transport to the Oceans. *Science* **2013**, *340*, 345−347. (b) Rhoades, C. C.; Chow, A. T.; Covino, T. P.; Fegel, T. S.; Pierson, D. N.; Rhea, A. E. The Legacy of a Severe Wildfire on Stream Nitrogen and Carbon in Headwater Catchments. *Ecosystems* **2019**, *22*, 643−657.
(49) Santos, F.; Wymore, A. S.; Jackson, B. K.; Sullivan, S. M. P.; McDowell, W. H.; Berhe, A. A. Fire severity, time since fire, and site-level characteristics influence streamwater chemistry at baseflow conditions in catchments of the Sierra Nevada, California, USA. *Fire Ecol.* **2019**, *15*, No. 3.
(50) Bostick, K. W.; Zimmerman, A. R.; Wozniak, A. S.; Mitra, S.; Hatcher, P. G. Production and Composition of Pyrogenic Dissolved Organic Matter From a Logical Series of Laboratory-Generated Chars. *Front. Earth Sci.* **2018**, *6*, No. 43.

https://doi.org/10.1021/acsestwater.3c00017
ACS EST Water 2023, 3, 2199−2209